Optical and Electrical Properties of Homo and Heterojunction Formed by the ZnO/FTO and CuO/ZnO/FTO Nanostructures

R. R. Ghimire, B. P. Pokhrel, S. P. Gupta, L. P. Joshi and K. B. Rai

Journal of Nepal Physical Society

Volume 9, Issue 1, June 2023

ISSN: 2392-473X (Print), 2738-9537 (Online)

JNPS, **9** (1): 73-82 (2023)

DOI: https://doi.org/10.3126/jnphyssoc.v9i1.57600

Published by:

Nepal Physical Society
P.O. Box: 2934
Tri-Chandra Campus
Kathmandu, Nepal
Email: nps.editor@gmail.com

JNPS 9 (1): 73-82 (2023)
ISSN: 2392-473X (Print), 2738-9537 (Online)

Research Article *© Nepal Physical Society*
DOI: https://doi.org/10.3126/jnphyssoc.v9i1.57600

Optical and Electrical Properties of Homo and Heterojunction Formed by the ZnO/FTO and CuO/ZnO/FTO Nanostructures

R. R. Ghimire[1], B. P. Pokhrel[1], S. P. Gupta[1], L. P. Joshi[2] and K. B. Rai[1, *]
[1]Department of Physics, Patan Multiple Campus, Tribhuvan University, Nepal
[2]Department of Physics, Amrit Science Campus, Tribhuvan University, Nepal
[*]Corresponding Email: krishnarai135@gmail.com

Received: *7th March, 2023;* ***Revised:*** *15th April, 2023;* ***Accepted:*** *24th June, 2023*

ABSTRACT

The most common materials used to create electrical and optoelectronic devices for a variety of applications including transistor, sensor and detector are semiconductor nanostructures. Combining the nanostructures can result semiconductor homostructure and heterostructure. The homojunction of ZnO/FTO and heterojucntion of CuO/ZnO/FTO coated glass substrate are formed using spray pyrolysis technique. The optical band gap for the FTO, ZnO, ZnO/FTO and CuO/ZnO/FTO films calculated using data from UV-visible spectroscopy are 3.629 eV, 3.236 eV, 3.113 eV and 1.456 eV respectively. The observed ohmic behavior of ZnO/FTO homojunction is due to the close band gap of FTO (i.e. E_g = 3.629 eV) and ZnO (E_g = 3.236 eV) whereas the non-ohmic behavior of CuO/ZnO/FTO heterojunction is due to the significant different in band gap energy of CuO (i.e. E_g = 1.456 eV) and ZnO (E_g = 3.236 eV). The photocurrent for ZnO/FTO homojunction increases from 232 µA to 350 µA for visible light illumination and from 232 µA to 400 µA for UV light illumination at bias voltage of 2.5 V. There is no significantly changed in the threshold voltage in visible region. For the CuO/ZnO/FTO heterojunction, the photocurrent increases from 280 µA to 390 µA for visible illumination and from 280 µA to 480 µA for UV illumination at 2.5 V. The enhancement of channel current in both sample (i.e. homojunction and heterojunction) under visible illumination is due to detrapping the charge carriers from mid gap states and released to the conduction band. The large enhancement of photocurrent under UV illumination is due to band gap absorption. Threshold voltage for CuO/ZnO/FTO non-ohmic device is shifted negatively from 1 V to 0 V with increasing the frequency of incident radiation. It suggests that the heterojunction formed by CuO/ZnO/FTO structure is applicable for broad band photo detector.

Keywords: Zinc oxide, Copper oxide, Fluorine doped tin oxide, Heterojunction, Photo response.

INTRODUCTION

One of the most common materials used to create electrical and optoelectronic devices for a variety of applications including transistor, sensor and detector is semiconductor nanostructures [1, 2]. These nanostructures can be combined to create a heterostructure semiconductor that can be utilized as a broad-band photodetector and a tool for understanding Scotty diode behavior [3]. Zinc oxide/Fluorine doped tin oxide (ZnO/FTO) and Copper oxide/Zinc oxide/Fluorine doped tin oxide (CuO/ZnO/FTO) nanostructures have attracted considerable attention due to their unique properties and potential applications in various fields, including optoelectronics, energy conversion and storage, sensors, and catalysis [4, 5]. ZnO is a wide-bandgap semiconductor with excellent optical and electrical properties, while CuO is a p-type semiconductor with good catalytic activity and gas sensing properties. The combination of these materials in a heterojunction can lead to interesting electronic and optical phenomena. These semiconducting materials have distinct unequal band gap energies and unequal Fermi level. The combination of multiple heterojunctions together in a device is called a heterostructure. A semiconductor junction's behavior is influenced by the alignment of the energy bands at the contact [6, 7]. Materials having very close band gap can show the homojunction at the interface [8]. Zinc oxide (ZnO) has been widely investigated as a promising material for light emitting devices, UV photo detectors, chemical and biological sensor [9-12]. The lack of p-type electrical conductivity in ZnO emphasizes the importance of the study of hybrid heterojunctions [13-15]. Among different type of materials, copper oxide is a good candidate to create heterojunctions with ZnO [16-18]. Copper oxide has two stable polymorphs: cuprous oxide (Cu_2O) and cupric oxide (CuO), both of them are of p-type conductivity in nature with the band gap ≈ 2.1 eV and ≈1.4 eV respectively [19]. Heterojunction formed by two different semiconductors such as CuO and ZnO has unique electrical and electro-optical properties. The most important differences between these materials are the energy gap. The difference of energy gap in these materials permits spatial confinement of injected electrons and holes. Fluorine doped tin oxide (FTO) has been recognized as a very promising material because it is relatively stable under atmospheric condition, excellent electrical conductivity, greater mobility, chemically inert, mechanically hard and high-temperature resistant [20, 21]. It has wide band gap semiconductor, high transmittance in the visible region and highly reflecting in the infrared region. It is also used in gas sensing materials [22]. Previous studies have reported on the synthesis and characterization of ZnO/FTO and CuO/ZnO/FTO nanostructures, as well as their optical and electrical properties. Munprom et al. synthesized ZnO/FTO nanowire arrays using a hydrothermal method and studied their optical and electrical properties. They found that the nanowires exhibited strong UV emission and good conductivity [23]. The synthesis of CuO, ZnO, FTO and their heterojunction of CuO/ZnO/FTO arrays demonstrated their gas sensing properties, photo-microbial fuel cell sensor for the detection of heavy metals and low turn-on voltage [5, 11, 18, 24, 25]. Despite the significant progress made in the synthesis and characterization of ZnO/FTO and CuO/ZnO/FTO nanostructures, there are still many unanswered questions and challenges in this field. The effects of visible and UV-Visible light on the optical and electrical properties of these materials are not well understood. The mechanisms underlying the formation and properties of the CuO/ZnO heterojunction are also not fully understood.

In this work, we have presented a cost-effective method for the preparation of zinc oxide (ZnO) and copper oxide (CuO) and their respective fabrication on fluorine doped tin oxide **(**FTO) i.e. ZnO/FTO and CuO/ZnO/FTO nanostructures. We have also studied the optical properties, current-voltage (I-V) measurements and the photoresponse of fabricated ZnO/FTO and CuO/ZnO/FTO interface. Overall, this study will contribute to a better understanding of the optical and electrical properties of ZnO/FTO and CuO/ZnO/FTO nanostructures and pave the way for their practical applications in various fields.

MATERIALS AND METHODOLOGY

The chemical methods are used for the sample solution preparation of FTO, ZnO, CuO. The chemical methods for preparing ZnO, FTO and CuO thin films offer several advantages in terms of simplified fabrication, precise control over film properties, cost-effectiveness, versatility, and environmental friendliness. These methods have significant importance in various applications where thin films with tailored properties are required, making them a crucial part of thin film fabrication techniques. For deposition/coating of thin films of various materials of ZnO/FTO and CuO/ZnO/FTO over glass substrate, the spray pyrolysis technique is employed. Since, the pyrolysis offers several advantages for deposition of thin films including versatility, low cost, high purity, conformal coating, customizable film properties, scalability and environmental friendliness. These advantages make pyrolysis a valuable technique for thin film deposition in various applications and it is widely used in research and industrial settings for fabricating thin films with tailored properties [26 - 30].

(1) Synthesis and deposition of FTO on glass substrate

(a) Glass substrates cleaning

The commercial microscopic slides of quartz glass having the length = 75±1 mm, breadth = 25±1 mm, thickness = 1.35±0.1 mm (Tking Glass Co. ltd) were properly cleaned with detergent and then with ultrasonically for 15 minutes using an ultrasonic cleaner (PS-60A, ROHS) prior to the preparation and deposition of FTO films. The substrates were then thoroughly dried to remove any remaining water droplets [26]. Again, these substrates were rinsed with distilled water, dried them for 15 minute and finally these were ready for deposition of FTO film.

(b) Preparation of precursor solution of FTO and its deposition/coating on glass substrate

For this, 15 gm of dehydrated tin chloride ($SnCl_2.2H_2O$) of Meghachem India with purity 97% was taken and mixed with 7 ml of conc. hydrochloric acid (HCl) of Sigma Aldrich Company with purity 99%. It was heated for 15 minute at 85 ºC together with the mixing of 30 ml of distilled water then stirred for 15 minute. In addition, for the preparation of solution of ammonium fluoride (NH_4F), 15.66 gm of NH_4F of Otto Chemie India with purity 98% was mixed with 37 ml of distilled water and then heated up to 60 ºC together with stirring for 15 minute. The precursor solutions of tin chloride and ammonium fluoride were then mixed with continuous stirring for 1 hour at room temperature for the preparation of FTO. The solution prepared was kept in 24 hour for aging. After this, thin film of FTO was deposited on cleaned glass substrate using the homemade spray pyrolysis experimental system in laboratory. In this spray pyrolysis technique, the normal distance at about 1-2 cm. between nozzle and glass substrate was fixed. The FTO liquid was then sprayed to the hot substrate such that the thin film of FTO deposition occurred [27]. The temperature for this deposition was set to 400 °C under the use of temperature controller.

(2) Preparation and deposition of ZnO thin film

0.5 M precursor solution was prepared using acetate route in which zinc acetate hydrate [$Zn(CH_3COO)_2.2H_2O$)] of Sigma Aldrich Company with purity 99.9% was mixed in distilled water and was stirred with the help of magnetic stirrer for 2 hour. This solution was kept in the ultrasonic nebulizer where delivery tube with spray nozzle was attached on it. The ZnO film was deposited on FTO coated glass substrate using home-made spray pyrolysis set up where controllable heating system was used to anneal the ZnO film at 400 °C [28].

(3) Synthesis of CuO, its solution preparation by dispersion method and CuO thin film deposition

Copper oxide was synthesized by the chemical precipitation method in which 0.5 M solution was prepared using the copper (II) chloride ($CuCl_2.2H_2O$) of Merck India with purity 99% and distilled water. Then sodium hydroxide (NaOH) of Merck India with purity 99.8% was added dropwise to already prepared 0.5 M solution and stirred continuously up to 30 minute until brown precipitate of $Cu(OH)_2$ occurred. This solution was now washed with distilled water for five time and subjected to centrifuge. After centrifuging, we got a brown solid particle which contained water and it was subjected to drying at 70 °C then heated with a high temperature of about 300 ºC then finally black CuO was obtained [29]. Here, figure 1 shows the flow chart of the procedure for synthesis of CuO.

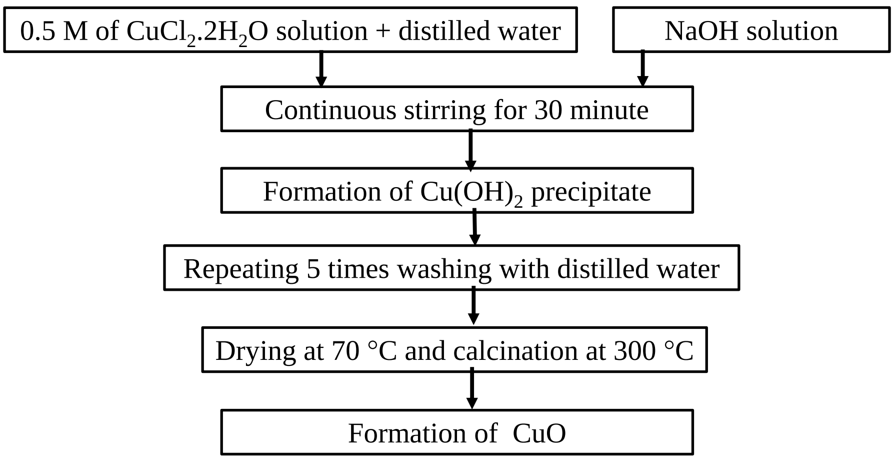

Fig. 1: The flow chart of the procedure for synthesis of CuO.

Small amount of CuO was added into Ethylene Glycol $(CH_2OH)_2$ of Merck India with purity 99.5% such that prepared CuO particles got dispersed [30] and then it was stirred for 1 hour at room temperature. Finally, it was deposited by spray pyrolysis method to make heterostructure between CuO and ZnO over FTO coated glass substrates. About 20 number of coat of CuO were made over ZnO on FTO coated glass substrates.

The UV-Visible spectroscopy with the wavelength range from 193 nm – 1117 nm at Amrit Science Campus was used for optical characterization and determine the band gap of FTO, ZnO, ZnO/FTO and CuO/ZnO/FTO. For I-V characterization, DC power supply of Scientech for voltage source with range 0 V to 30 V was used and current was measured using Fluke multimeter.

The properties of homo-structure and heterostructure depend on various fabrication parameters such as the thickness of the layers, the doping levels of the materials and the device geometry. Detailed characterization and optimization of these parameters are required to achieve desired performance in ZnO/FTO homojunction and CuO/ZnO/FTO heterojunction devices coated on glass substrates.

RESULT AND DISCUSSIONS

The schematic figures 2(a) and 2(b) show the circuits where the voltmeter and microammeter were used for the I-V measurement of homo and heterojunction nanostructures.

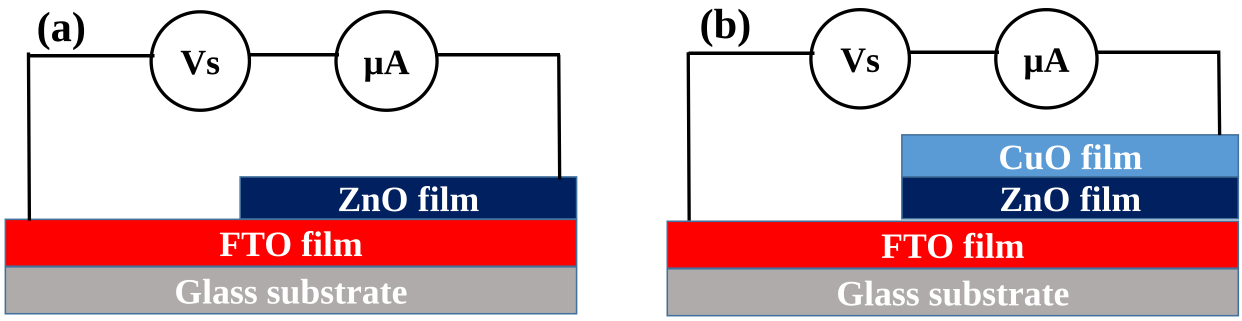

Fig. 2: Schematic diagram of current (I) –voltage (V) measurement of (a) ZnO/FTO homojunction (b) CuO/ZnO/FTO heterojunction.

Optical Properties:

To study the optical properties of FTO, ZnO, ZnO/FTO and CuO/ZnO/FTO, the optical band gap obtained from measured transmittance has been determined using the Tauc relation $(\alpha h\nu)^{\frac{1}{r}} = A(h\nu - E_g)$ [26] where α is the optical absorption coefficient, h is Planck's constant, ν is the photon frequency, A is energy independent constant and E_g is optical band gap. Figure 3 is the plotting of the graph between $(\alpha h\nu)^{\frac{1}{r}}$ versus photon energy (hν) where the photon energy (hν) is obtained from the wavelength using the relation, $h\nu = \frac{1240}{\text{wavelength}}$. The power factor (r) takes the values of $\frac{1}{2}, 2$ for allowed direct and allowed indirect band transition respectively. Here, the materials FTO, ZnO, ZnO/FTO and CuO/ZnO/FTO have direct band transition.

Figure 3 shows the band gap of (a) FTO (b) ZnO (c) ZnO/FTO (d) CuO/ZnO/FTO. The optical band gap of the different films calculated from wavelength and transmittance/absorption data obtained from UV-Visible Spectroscopy for FTO is 3.629 eV, ZnO is 3.236 eV, ZnO/FTO is 3.113 eV and CuO/ZnO/FTO is 1.456 eV. For the FTO and ZnO, they have comparable band gap energy and hence form the homojunction between ZnO and FTO. The optical properties of the ZnO/FTO homojunction, such as transmittance and reflectance are studied to understand how the materials interact with light. High transmittance and low reflectance in the visible and near-infrared regions are desirable for efficient solar cell performance [23]. The value of band gap of CuO is 1.4 eV [19] which is far from the value of the band gap of ZnO i.e. 3.236 eV. Due to the difference in value of band gap between CuO and ZnO, they form heterojunction.

Here, a layer of zinc oxide (ZnO) is sandwiched between layers of copper oxide (CuO) and fluorine-doped tin oxide (FTO). The properties of the interfaces between CuO/ZnO and ZnO/FTO layers are crucial for the performance of the heterojunction. Studies in the literature have reported that the band alignment and energy level alignment at the interfaces play a significant role in determining the charge separation, transport and collection processes. Properly aligned energy levels and favorable band offsets can lead to enhance the device performance [11, 18, 25].

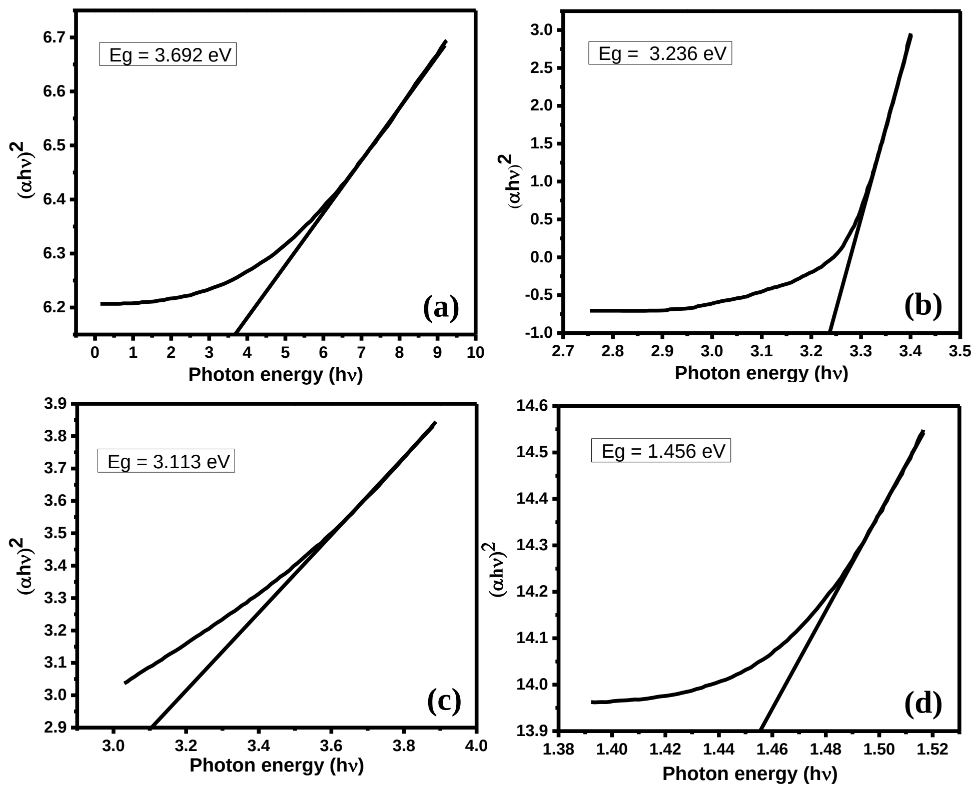

Fig. 3: plot of band gap of (a) FTO (b) ZnO (c) ZnO/FTO (d) CuO/ZnO/FTO.

Electrical Properties:

Homojunction of ZnO/FTO

Figure 4(a) contains I-V characteristics of ZnO/FTO homojunction and this is achieved due to comparable band gap energy between ZnO and FTO. The ohmic behavior of homojunction in this figure can be analyzed by the linear fitting (red color line) with correlation values of 0.99 in the figure 4(b). Figure 4(a) shows that the symmetric behavior of current and voltage in which value of current is nearly same as 500 μA corresponding to 2.5 V supplied on forward and reverse biased. This symmetricity is due to the nearly equal fermi level and refractive index [1-3, 6, 25, 31-33]. The electron affinity of the ZnO and FTO is also nearly equal so that nano-composite between two films unable to form a heterojunction.

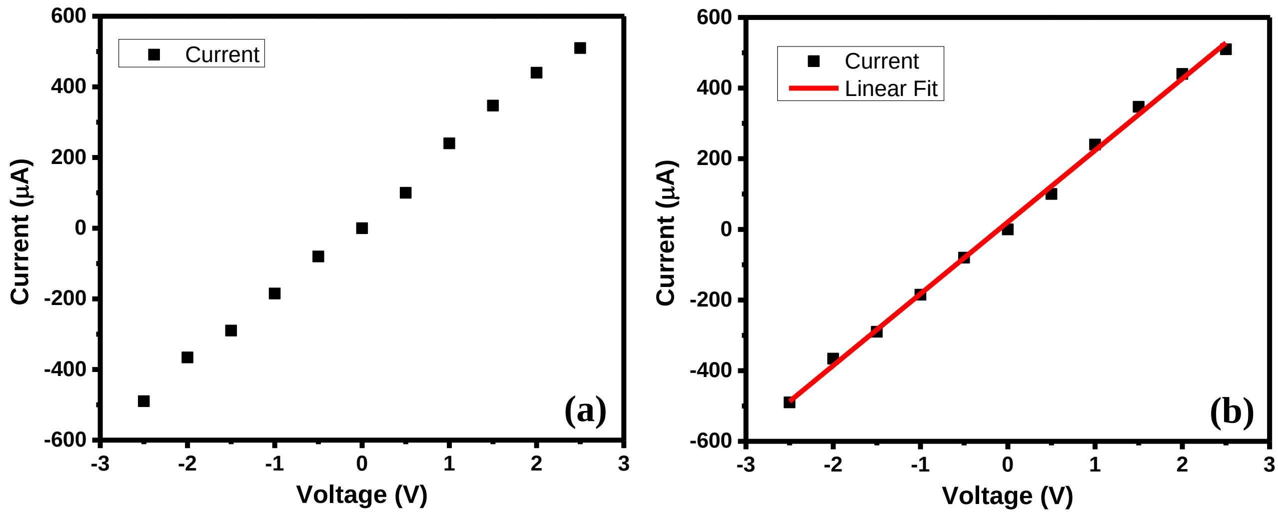

Fig. 4: (a) I-V characteristics of ZnO/FTO homojunction
(b) Linear fitting of I-V measurement of homojunction ZnO/FTO.

Heterojunction of CuO/ZnO/FTO

Figure 5 shows the non-ohmic current voltage relation formed after the deposition of CuO particle by dispersing in Ethylene Glycol. When CuO film is deposited over ZnO film, there exist interface between ZnO and CuO films and then rectifying property is occurred. This type of diode is called schottky diode. It gives the non-ohmic behavior of current voltage relation of CuO/ZnO on FTO coated glass substrates. Non-ohmic behavior is formed due to the schottky barrier and it is occurred at the interface. Schottky barrier arises due to the difference in band gap energy and refractive index [31-33]. At the interface of CuO/ZnO heterostructure, the internal electric field is generated due to difference in fermi levels and as a result, the reverse transfer of electrons and holes across heterostructure interface can be easily achieved. Hence, on the basis of this favorable electronic structure, CuO/ZnO on FTO exhibits better performance of schottky diode.

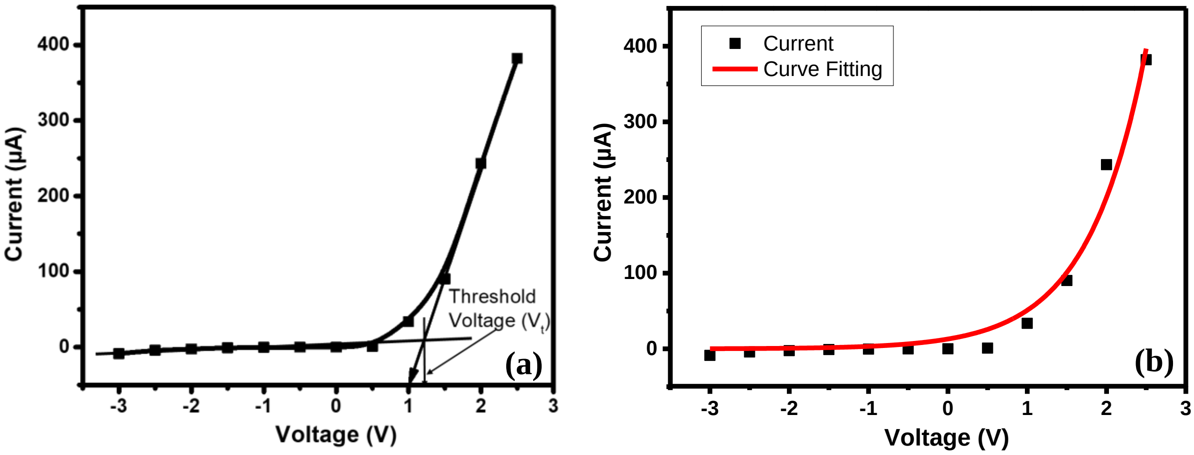

Fig. 5: (a) I-V measurement of heterojunction CuO/ZnO on FTO
(b) curve fitting of I-V measurement of heterojunction CuO/ZnO on FTO.

Figure 5(b) is the fitting curve of the I-V measurement of heterojunction CuO/ZnO on FTO. When the diode equation for figure 5(a) is fitted by using exponential function, we get the figure 5(b).

We know that the standard diode equation $I = I_s\left[e^{\left(\frac{V}{\eta V_t}\right)} - 1\right]$, Where, η is the ideality factor and its value is assumed to 1 [34], I_s is the saturation current and V_t is the threshold voltage. The equivalent equation with standard diode equation is $y = ae^{bx}$. Now, comparing the equivalent diode equation with the standard diode equation, the value of 'a' and the value of 'b' represent the saturation current (I_s) and threshold voltage (V_t) respectively. These show that the saturation current and threshold voltage are 12.98 μA ± 3.63 μA and 1.36 V ± 0.11 V (experimentally nearly 1.2 V) respectively with correlation values of 0.97. The correlation values near to 1 shows good fit [35]. The fitted curve is better at the 0.05 significance level.

Photo-response of homo and heterojunction

It is worth mentioning that I-V characteristics measurement are used for the analysis of performances of photo devices. In lab, it has been done for the response of different color of light on ohmic devices made up from ZnO/FTO homojunction and non-ohmic devices made up from CuO/ZnO/FTO heterojunction.

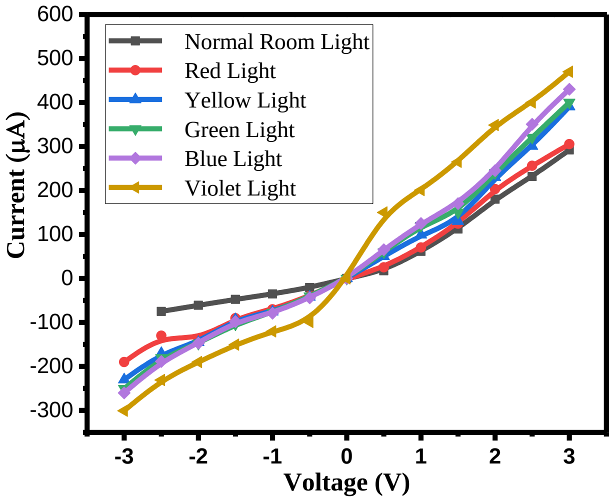

Fig. 6: I-V measurement or photo response properties of ZnO/FTO homojunction.

Figure 6 shows the photo response of ohmic devices. It shows slightly change in channel current with different color of light. This device is more sensitive in violet light than other visible light because of the absence of CuO film. The photocurrent for ZnO/FTO homojunction increases from 232 µA to 350 µA for visible light illumination and from 232 µA to 400 µA for UV light illumination at bias voltage of 2.5 V. There is no significantly changed in the threshold voltage in visible region.

When a small amount of external energy in the form of light with energy greater or equal with E_g of semiconductor is applied, the valence electrons gain enough energy to break the bonding with the parent atom and they jumps into the conduction band [29, 36]. Hence, they move freely from one place to another place. If the light energy applied on the semiconductor is further increased then more number of free electron are generated. Thus, electric current in the semiconductor increases with the increase in the light energy with decreasing threshold voltage [36]. The different color of light i.e. red, yellow, green, blue, violet have different wavelength ranges from 380-750 nm. From figure 6, red light shows less photo response than violet light because high wavelength of light has less penetration power to the material and by then only upper surface of sample is affected by the red light. This is the reason that no more current is increased. But in case of violet light, it has less wavelength and high penetration power so this light can influence up to depth in semiconducting film which ultimately shows good photo-response. On the other hand, band gap of ZnO/FTO junction is 3.113 eV which is nearly equal with the energy of the violet light so here violet light is only able to increase little more current than other color of light which is shown in figure 6.

Therefore, after the illumination of visible light (i.e. from normal to blue light) towards ZnO/FTO homojunction, there is small change in photocurrent i.e. 118 µA whereas in case of UV illumination, the current is increased by 168 µA. The increase in current in case of UV illumination is due to the comparable band gap of ZnO with energy of UV light. Optimizing device parameters of ZnO/FTO can help tailor the photoresponse characteristics of the device including overall performance.

Figure 7 shows the photo response of different color of light on non-ohmic device made up from CuO/ZnO on FTO substrates.

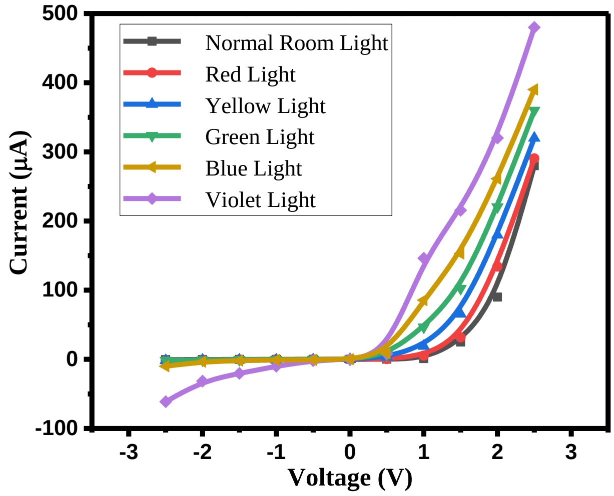

Fig. 7: I-V measurement or photo response properties of CuO/ZnO/FTO heterojunction.

Here, the band gap of CuO/ZnO/FTO heterostructure has 1.456 eV which corresponds to the wavelength of 840 nm. Under the illumination of different color of light, the threshold voltage sufficiently decreases towards negative bias and has enough energy to increase current in heterojunction. Threshold voltage for non-ohmic device is shifted negatively from 1 V to 0 V with increasing the frequency of incident radiation. The negative shift of threshold voltage is due to the increase in carrier concentration by optical illumination from visible to UV regions [37]. The photocurrent increases from 280 µA to 390 µA for visible illumination and from 280 µA to 480 µA for UV illumination at 2.5 V. The value of channel current is monotonically increases in CuO/ZnO/FTO heterojunction under illumination rather than the homojunction ZnO/FTO due to the band gap of CuO which lies in longest visible region (850 nm). The enhancement of channel current in both sample (i.e. homojunction and heterojunction) under visible illumination is due to detrapping the charge carriers from mid gap states and released to the conduction band. The large enhancement of photocurrent under UV illumination is due to band gap absorption. The photocurrent increases with increasing the light frequency. Higher the frequency, higher the energy and the violet light is very close to the fundamental band gap of ZnO which helps to generate the electron from valence band to the conduction band. Similarly CuO film is more sensitive with visible illumination because its band gap lies in this region i.e. the photo response in visible region primarily arises due to the fundamental band gap of CuO lies in this region. From figure 7, light with high wavelength shows less photoresponse than violet light, it is because with decreasing the wavelength, photon energy will increase which generates a large number of charge carriers in the conduction band. With increasing the charge carriers, a threshold voltage will shift negatively particularly for CuO/ZnO/FTO heterojunction. So, CuO/ZnO/FTO heterostructure can be used as broad band photo detector from visible to UV region. The low band gap of CuO and wide band gap of ZnO leads to the change in photocurrent for heterojunction CuO/ZnO/FTO in visible to UV region.

The close band gap of the ZnO/FTO homojunction allows for efficient charge transport in both directions while the significant difference in band gap energy of the CuO/ZnO/FTO heterojunction results in unique behavior, including efficient charge separation and transport, a built-in electric field and potentially higher light absorption which can impact its performance in photodetection and other optoelectronic applications [5, 11, 18, 23, 25, 36].

The CuO/ZnO/FTO heterojunction structure has promising potential for photo detection applications such as photovoltaic cells, UV sensors, photodetectors, optical switches, imaging devices and further research and development are needed to fully explore and optimize its performance in various device configurations and applications. The CuO/ZnO/FTO heterojunction structure offers several advantages. The heterojunction structure allows for efficient charge separation and collection at the CuO/ZnO interface leading to improve performance in terms of photocurrent generation, photoresponsivity and response times. The CuO and ZnO layers can be easily deposited using various techniques such as chemical solution deposition, sputtering, or atomic layer deposition, making it compatible with different fabrication processes [11, 16-19, 24, 25, 36].

CONCLUSION

Homojunction and heterojuction devices were fabricated based on ZnO and CuO nanostructured film on FTO coated glass substrate by spray pyrolysis technique. Using Tauc plot, optical band gap of FTO, ZnO, ZnO/FTO and CuO/ZnO/FTO were found as 3.629, 3.236, 3.113 and 1.456 eV respectively. The comparable band gap energy between ZnO and FTO showed the ohmic behavior with symmetric current voltage relation of homojunction of them. The non-ohmic behavior of current voltage relation was obtained on CuO/ZnO/FTO heterostructure by the formation of schottky barrier at the interface due to the difference in band gap energy. The fitted curve for the non-ohmic behavior of CuO/ZnO/FTO showed that the saturation current and threshold voltage are 12.98 µA ± 3.63 µA and 1.36 V ± 0.11 V respectively with correlation values of 0.97. The photocurrent for ZnO/FTO homojunction increases from 232 µA to 350 µA for visible light illumination and from 232 µA to 400 µA for UV light illumination at bias voltage of 2.5 V. There is no significantly changed in the threshold voltage in visible region. For the CuO/ZnO/FTO heterojunction, the photocurrent increases from 280 µA to 390 µA for visible illumination and from 280 µA to 480 µA for UV illumination at 2.5 V. The value of channel current is monotonically increases in CuO/ZnO/FTO heterojunction under illumination rather than the homojunction ZnO/FTO due to the band gap of CuO which lies in longest visible region (850 nm). The enhancement of channel current in both sample (i.e. homojunction and heterojunction) under visible illumination is due to detrapping the charge carriers from mid gap states and released to the conduction band. The large enhancement of photocurrent under UV illumination is due to band gap absorption. Threshold voltage for non-ohmic device is shifted negatively from 1 V to 0 V with increasing the frequency of incident radiation. The negative shift of threshold voltage is due to the increase in carrier concentration by optical illumination. This CuO/ZnO/FTO heterojunction is particularly useful in schottky diode and broadband photo detection applications.

Optical and electrical properties of ZnO/FTO and CuO/ZnO/FTO nanostructures can provide valuable insights and there are some limitations too such as limited parameter space, specific doping concentrations, fabrication methods, defects and impurities, interface effects, temperature effects and practical device performance that should be considered. Addressing these limitations and conducting further research in these areas could enhance our understanding of the properties and potential applications of these nanostructures. Investigating the effects of environmental factors such as temperature, humidity and light exposure, on the optical and electrical properties of ZnO/FTO and CuO/ZnO/FTO nanostructures, can be future research work and it can provide understanding about experiments under different environmental effects that can help in optimizing the performance and reliability of the nanostructures for practical applications.

REFERENCES

[1] Ding, M.; Guo, Z.; Zhou, L.; Fang, X. and Zhang, L. et al. "One-Dimensional Zinc Oxide Nanomaterials for Application in High-Performance Advanced Optoelectronic Devices," *Crystals*, **8** (5): 223 (1-29) (2018).

[2] Sharma, D. K.; Shukla, S.; Sharma, K. K. and Kumar. V. "A review on ZnO: Fundamental properties and applications," *Materials Today: Proceedings*, **49** (2): 3028-3035 (2022).

[3] Wali, S.; Yin, Q.; Si, J. G.; Shafi, M. and Ren, J. et al. "Organic rubrene/topological insulator Bi_2Se_3/SiO_2 hybrid heterojunction photodetectors for broadband and ultrafast photodetection application," *Journal of Materials Chemistry C*, **10**: 1289-1301 (2022).

[4] Zhang, S. T.; Vitrant, G.; Pernot, E.; Jimenez, C.; Munoz-Rojas, D. and Bellet, D. "Hazy Al_2O_3-FTO Nanocomposites: A Comparative Study with FTO-Based Nanocomposites Integrating ZnO and S:TiO_2 Nanostructures" *Nanomaterials*, **8** (6); 440 (2018).

[5] Lu, Y.; Hu, X.; Tang, L.; Peng, B. and Tang, J. et al. "Effect of CuO/ZnO/FTO electrode properties on the performance of a photo-microbial fuel cell sensor for the detection of heavy metals" *Chemosphere*, **302:** 134779 (2022).

[6] Chen, J.; Ouyang, W.; Yang, W.; He, J. H. and Fang, X. "Recent Progress of Heterojunction Ultraviolet Photodetectors: Materials, Integrations, and Applications," *Advanced Functional Materials*, **30** (16): 1909909(1-18) (2020).

[7] Shrestha, S. P.; Ghimire, R. R.; Nakarmi, J. J.; Kim, Y. S. and Shrestha, S. "Properties of ZnO:Al Films Prepared by Spin Coating of Aged Precursor Solution," *Bulletin of the Korean Chemical Society*, **31** (1): 112-115 (2010).

[8] Ali, N.; Ahmed, R.; Luo, J. T.; Wang, M. and Kalam, A. et al. "Advances in nanostructured homojunction solar cells and photovoltaic materials," *Materials Science in Semiconductor Processing*, **107**: 104810 (1-9) (2020).

[9] Ghimire, R. R.; Parajuli, A.; Gupta, S. P. and Rai, K. B. "Synthesis of ZnO Nanoparticles by Chemical Method and its Structural and Optical Characterization," *Bibechana*, **19** (1-2): 90-96, (2022).

[10] Ghimire, R. R.; Dahal, Y. P.; Rai, K. B. and Gupta. S. P. "Determination of Optical Constants and Thickness of Nanostructured ZnO Film by Spin Coating Technique," *Journal of Nepal Physical Society*, **7** (2): 119-125 (2021).

[11] Yatskiv, R.; Tiagulskyi, S.; Grym, J.; Vanis, J. and Bašinova, N. et al. "Optical and electrical characterization of CuO/ZnO heterojunctions," *Thin Solid Films*, **693**: 137656 (2020).

[12] Wang, Z. L. "Zinc oxide nanostructures: growth, properties and applications," *Journal of Physics: Condensed Matter*, **16** (25): R829–R858 (2004).

[13] Janotti, A. and Van de Walle, C. G. "Fundamentals of zinc oxide as a semiconductor," *Reports on Progress in Physics*, **72** (12): 126501 (2009).

[14] Look, D. C. and Claflin, B. "P-type doping and devices based on ZnO," *Physica status solidi (b)*, **241** (3): 624-630 (2004).

[15] Reynolds, J. G. and Reynolds, C. L. "Progress in ZnO Acceptor Doping: What Is the Best Strategy?," *Advances in Condensed Matter Physics*, **2014**: 457058(1-15) (2014).

[16] Wong, T. K. S.; Zhuk, S.; Masudy-Panah, S. and Dalapati, G. K. "Current Status and Future Prospects of Copper Oxide Heterojunction Solar Cells," *Materials* **9** (4): 271(1-21) (2016).

[17] Miller, D. R.; Akbar, S. A. and Morris, P. A. "Nanoscale metal oxide-based heterojunctions for gas sensing: A review," *Sensors and Actuators B: Chemical*, **204**: 250-272 (2014).

[18] Oliveiraa, M. C.; Fonseca, V. S.; Andrade Neto, N. F.; Ribeiro, R. A. P. and Longo, E. et al. "Connecting theory with experiment to understand the photocatalytic activity of CuO–ZnO heterostructure," *Ceramics International*, **16** (7): 9446-9454 (2020).

[19] Meyer, B. K.; Polity, A.; Reppin, D.; Becker, M. and Hering, P. et al. "Binary copper oxide semiconductors: From materials towards devices," *Physics Status Solidi (b)*, **249**: 1487-1509 (2012).

[20] Thangaraju, B. "Structural and electrical studies on highly conducting spray deposited fluorine and antimony doped SnO_2 thin films from $SnCl_2$ precursor," *Thin Solid Films*, **402** (1-2): 71-78 (2002).

[21] Ghimire, R. R.; Dahal, Y. P. and Rai, K. B. "Fabrication of UV sensing transistor based on transparent polycrystalline zinc oxide thin film using polymeric electrolyte gate dielectric," *Bibechana*, **20** (1): 46-54 (2023).

[22] Kawashima, T.; Ezure, T.; Okada, K.; Matsui, H. and Goto, K. et al. "FTO/ITO double-layered transparent conductive oxide for dye-sensitized solar cells," *Journal of Photochemistry and Photobiology A: Chemistry*, **164**: 199-202 (2004).

[23] Munprom, R.; Sae-tiaw, C.; Phiankoh, S.; Jongprateep, O. and Surawathanawises. K. et al. "Structural, optical, and electrical modification of hydrothermally grown ZnO nanorods by tin-doping," *Materials Research Express*, **6**: 095916 (2019).

[24] Li, D.; Qin, L.; Zhao, P.; Zhang, Y. and Liu, D. et al. "Preparation and gas-sensing performances of ZnO/CuO rough nanotubular arrays for low-working temperature H_2S detection" *Sensors and Actuators B: Chemical*, **254**: 834-841 (2018).

[25] Lopez, R.; Villa-Sanchez, G.; Vivaldo de la Cruz, I.; Encarnacion-Gomez, C. and Castrejon-Sanchez, V. H. et al. "Cupric oxide (CuO)/zinc oxide (ZnO) heterojunction diode with low turn-on voltage," *Results in Physics*, **22**: 103891(1-10), (2021).

[26] Yadav, R. P.; Rai, K. B. and Shrestha, S. P. "Electrical and optical properties of dip coated Al-doped ZnO thin films: Effect of Al-concentration, starting solution and sample ageing," *Mongolian Journal of Chemistry*, **22** (48): 38-44 (2021).

[27] Lefdil, M. A.; Diaz, R.; Bihri, H.; Aouaj, M. A. and Rueda, F. "Preparation and characterization of sprayed FTO thin films," *The European Physical Journal-Applied Physics*, **38** (3): 217-219 (2007).

[28] Shinde, S. S.; Bhosale, C. H. and Rajpure, K. Y. "Structural, optical, electrical and thermal properties of zinc oxide thin films by chemical spray pyrolysis," *Journal of Molecular Structure*, **1021**: 123-129 (2012).

[29] Jia, D.; Yu, J. and Xia, X. "Synthesis of CuO nanometer powder by one step solid state reaction at room temperature," *Chinese Science Bulletin*, **43**: 571-573 (1998).

[30] Reverberi, A. P.; Salerno, M.; Lauciello, S. and Fabiano, B. "Synthesis of Copper Nanoparticles in Ethylene Glycol by Chemical Reduction with Vanadium (+2) Salts", *Materials*, **9** (10): 809 (2016).

[31] Ching-Prado, E.; Watson, A.; Miranda, H. "Optical and electrical properties of fluorine doped tin oxide thin film," *Journal of Materials Science: Materials in Electronics*, **29** (5): 15299-15306 (2018).

[32] Robertson, J. and Chen, C. W. "Schottky barrier heights of tantalum oxide, barium strontium titanate, lead titanate, and strontium bismuth tantalite," *Applied Physics Letters*, **74** (8): 1168-1170 (1999).

[33] Peacock, P. W. and Robertson, J. "Band offsets and Schottky barrier heights of high dielectric constant oxides," *Journal of Applied Physics*, **92** (8): 4712-4721 (2002).

[34] Kim, C. H.; Yaghmazadeh, O.; Bonnassieux, Y. and Horowitz, G. "Modeling the low-voltage regime of organic diodes: Origin of the ideality factor," *Journal of Applied Physics*, **110** (9): 093722-8 (2011).

[35] Osorio-Arrieta, D. L.; Munoz-Mata, J. L.; Beltran-Perez, G.; Castillo-Mixcoatl, J. and Mendoza-Barrera, C. O. et al. "Reduction of the Measurement Time by the Prediction of the Steady-State Response for Quartz Crystal Microbalance Gas Sensors," *Sensors*, **18** (8): 2475(2-12) (2018).

[36] Ghosh, A. and Mondal, A. "Fabrication of stable, efficient and recyclable p-CuO/n-ZnO thin film heterojunction for visible light driven photocatalytic degradation of organic dyes," *Materials Letters*, **164**: 221-224 (2016).

[37] Mondal, S.; Ghimire, R. R. and Raychaudhuri, A. K. "Enhancing photoresponse by synergy of gate and illumination in electric double layer field effect transistors fabricated on n-ZnO," *Applied Physics Letters*, **103**: 231105-5 (2013).